CONVERGING MOTION OF Hα CONJUGATE KERNELS: THE SIGNATURE OF FAST RELAXATION OF A SHEARED MAGNETIC FIELD

HAISHENG JI,[1,2] GUANGLI HUANG,[1] HAIMIN WANG,[2] TUANHUI ZHOU,[1] YOUPING LI,[1] YANAN ZHANG,[1] AND MUTAO SONG[1]

ABSTRACT

In this Letter, we present the results from a high-cadence (∼40 ms) Hα blue-wing observation of an M1.1-class solar flare, which occurred in NOAA AR 10687 on 2004 November 1. In collaboration with *RHESSI*, the observation was made with the Hα Fine Structure Telescope at the GanYu Solar Station of the Purple Mountain Observatory. For this flare, a pair of conjugate Hα kernels shows a kind of converging motion during the impulsive phase. After the impulsive phase, there appears a normal separation motion. The motion of one Hα kernel is perpendicular to the magnetic neutral line, while another kernel's converging shows both perpendicular and parallel components. Nevertheless, the shear angle decreases during the converging motion, clearly showing the relaxation of a sheared magnetic field. All of the above features are confirmed with hard X-ray (HXR) footpoints observed by *RHESSI*. We also obtained the time profiles of the rate of change of the shear angle and the relative velocity of the two kernels with Hα observations. Both of these time profiles show a good correlation with *RHESSI* HXR light curves in the higher energy range (≳50 keV). This indicates that, during the peak times of the flare, the relaxation process may have occurred rapidly. This event was also observed by the Nobeyama Radio Heliograph (NoRH), showing a single microwave source. Using NoRH maps at 17 GHz with 1 s cadence, we obtained the time profile of the radio source's velocity using the same method that we used with Hα images. The velocity-time curve of the microwave source shows a good correlation with that obtained from the two Hα kernels.

Subject headings: Sun: activity — Sun: flares — Sun: magnetic fields

1. INTRODUCTION

It is well accepted that solar flares are due to the sudden release of magnetic energy by magnetic reconnection (Priest & Forbes 2000). In the classical two-dimensional "CSHKP" reconnection model of a two-ribbon flare (Carmichael 1964; Sturrock 1966; Hirayama 1974; Kopp & Pneuman 1976), oppositely directed magnetic field lines are stretched by eruption to form a vertical current sheet where reconnection occurs. According to this model, the two footpoints (FPs) of a flare, residing in areas of opposite magnetic polarities, are expanding outward and away from each other as the flare proceeds (Švestka & Cliver 1992). Furthermore, it is well recognized that flare ribbon expansion is the chromospheric signature of progressive magnetic reconnection in the corona, in which new field lines reconnect at higher and higher altitudes. This picture, together with a simplified MHD reconnection model, yields a simplified method of measuring the electric field in the reconnection region. The product of the horizontal velocity of the ribbon expansion and local longitudinal magnetic field is a measure of an effective electric field strength along the current sheet (Forbes & Lin 2000 and references therein). The value of the effective electric field is usually taken as a measure of the reconnection rate. Meanwhile, the behaviors of hard X-ray (HXR) and/or Hα FPs are often used to infer the reconnection scenario during flares.

From the high-cadence and high spatial resolution observation of a C9.0 flare, Qiu et al. (2002) inferred the macroscopic electric field from the velocity of flaring kernels' motion and the longitudinal magnetic field. The temporal variation of the electric field inferred from one type of kernel motion is found to be correlated with HXR light curves during the rising phase of the flare. Wang et al. (2003) presented a detailed study of a two-ribbon flare and found evidence supporting the picture that an impulsive flare energy release is governed by fast magnetic reconnection in the solar corona. Other measurements of the reconnecting rate or of the electric field during large two-ribbon events have been attempted by Fletcher & Hudson (2001), Saba et al. (2001), and Asai et al. (2004). All of the results mentioned above seem to support the scenario of magnetic energy being released by current dissipation inside the current sheet.

The patterns of HXR FP motions observed by the Hard X-ray Telescope (HXT) on board *Yohkoh* were statistically investigated by Sakao et al. (1998). They reported that the separation between FPs does not always increase during flares. On the contrary, the separation is shown to be decreasing or is kept nearly unchanged for some flares. Somov et al. (2005) and Bogachev et al. (2005) analyzed 72 flares, and they concluded that there are three kinds of motion patterns for FPs. Most of the moving patterns cannot be explained with a simplified two-dimensional flaring model.

With high temporal and spatial resolution, the results of *RHESSI* observations (Fletcher & Hudson 2002; Krucker et al. 2003; Grigis & Benz 2005) have revealed more complex FP motion patterns than before. In addition, with the high-cadence observation of Hα blue-wing images, Ji et al. (2004) found a kind of converging motion of two conjugate Hα kernels during the impulsive phase of the 2002 September 9 flare. During the period of the converging motion, the single HXR loop-top source moves down. This kind of tendency of movement cannot be explained by the conventional simplified two-dimensional flare models (e.g., the "CSHKP reconnection model"). Certainly, we need further observational analysis for this kind of motion pattern with high-cadence observations.

[1] GanYu Solar Station, Purple Mountain Observatory, 2 Beijing Xi Lu, Nanjing 210008, China; jihs@mail.pmo.ac.cn.
[2] Big Bear Solar Observatory, New Jersey Institute of Technology, 40386 North Shore Lane, Big Bear City, CA 92314.
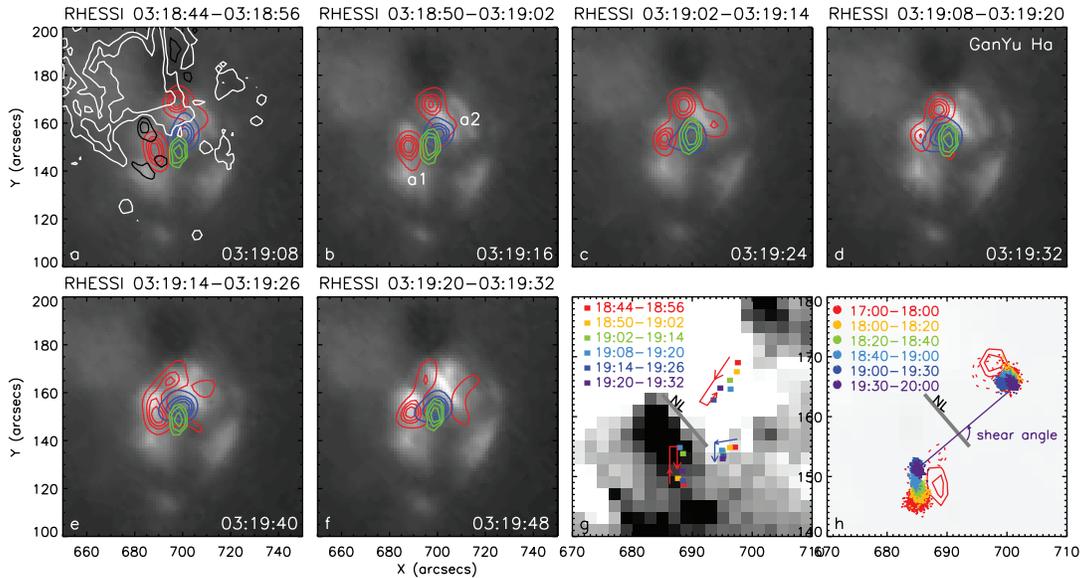
FIG. 1.—(a–f) Hα images of the flare observed at the GanYu Solar Station of the Purple Mountain Observatory. The white and black contours in panel a represent positive and negative longitudinal magnetic fields, respectively, as observed by MDI/SOHO. The red and blue contours are RHESSI maps in the energy range of 25–60 and 3–8 keV, respectively. The green contours are NoRH maps at 17 GHz. (g) Positions of HXR footpoint and loop-top sources at different times with respect to the neutral line. (h) Positions of the centroids of Hα kernels at different time periods. The solid and dotted contours are HXR emissions (25–60 keV) during the time intervals of 18:44–18:56 and 19:02–19:14, respectively.

2. OBSERVATION

In collaboration with the space observation made by the *Reuven Ramaty High Energy Solar Spectroscopic Imager* (*RHESSI*; Lin et al. 2002), we carried out ground-based high-cadence flare observations at Hα − 0.5 Å using the 26 cm Hα Fine Structure Telescope at the GanYu Solar Station of the Purple Mountain Observatory. The telescope is equipped with a CCD camera (659 × 494) running with a cadence of about 40 ms. The pixel size is 1″.13, which gives a field of view of about 745″ × 568″. The initial brightenings in the Hα blue wing are generally regarded as being suitable for locating non-thermal electron precipitation sites (Canfield & Gayley 1987). The reason for observing at Hα near off-band (−0.5 Å) instead of farther away from line center is that we need enough photon counts during small flares since, for NOAA AR 10687, major events were unlikely according to forecasting. On 2004 November 1, we observed an M1.1 flare in the active region. For this flare, the GanYu Hα telescope had a coverage from 03:17 to 03:20 UT.

RHESSI had a good coverage for this event. *RHESSI* was designed to investigate particle acceleration and energy release in solar flares, through imaging and spectroscopy of hard X-ray/gamma-ray continua emitted by energetic electrons and ions. The spatial resolution is as fine as ∼2″.3, and the time resolution for constructing images with sufficient counts is several seconds. This allows us to study the detailed moving features of HXR sources, as many authors have done (e.g., Sui & Holman 2003; Krucker et al. 2003). We use the CLEAN (Hurford et al. 2002) reconstruction algorithm to make HXR maps. The flare was also observed by the Nobeyama Radio Heliograph (NoRH), which is a well-known radio imaging instrument with a spatial resolution of 10″ at 17 GHz and a time resolution of 1 s (Nakajima et al. 1994).

3. RESULTS

The HXR light curves are plotted in Figures 2a and 2f below. According to the light curves, we may divide the whole flaring

process into two time intervals, I and II, which correspond to two main energy releasing periods.

The time sequences of the Hα images of the flare are shown in Figures 1a–1f. There are two flaring kernels: a1 and a2. As we can see in Figure 1a, kernels a1 and a2 belong to two opposite magnetic polarity regions. As seen from the movie that is made of the Hα images,[3] we found that the motion of kernel a1 is very obvious while a2 is almost motionless. This is similar to the 2000 March 16 flare investigated in detail by Qiu et al. (2002), for which only kernel k1 has a significant motion. We may define kernel a1 as the dynamic kernel. Being notable from the movie, kernel a1 moves toward a2 during the impulsive phase of the flare. With background-subtracted images, we computed the positions of the centroids of both conjugate kernels using the center-of-mass method (Ji et al. 2004).

The distance between the two Hα kernels as a function of time is plotted in Figure 2b, from which we can see that the distance decreases during the rising phase of HXR emissions. After the rising phase, the kernels have a separation motion. The white curve overlaid in Figure 2b is the smoothed curve using 101-point (∼4 s) averaging. The time derivative of the smoothed curve gives the relative velocity of the two Hα kernels as shown in Figure 2g. During the converging motion, the velocity-time curve shows two impulsive increases, which are well correlated with periods I and II mentioned above. Actually, it shows a better correlation with the HXR light curve in the higher energy range (≳50 keV).

We constructed HXR maps in the energy range of 3–8 keV (*blue contours*, Fig. 1) and 25–60 keV (*red contours*). We divided the time interval of 03:18:00–03:21:00 into a number of time bins; each bin has a duration of 12 s and overlaps the other by 6 s. The reason for selecting the bin size in such a way was to get sufficient counts and sufficient temporal resolution. HXR FP emissions appear only during the period of 03:18:30–03:19:30. During this period, *RHESSI* maps show a classical morphology of a flare in HXR: a loop-top source in

---

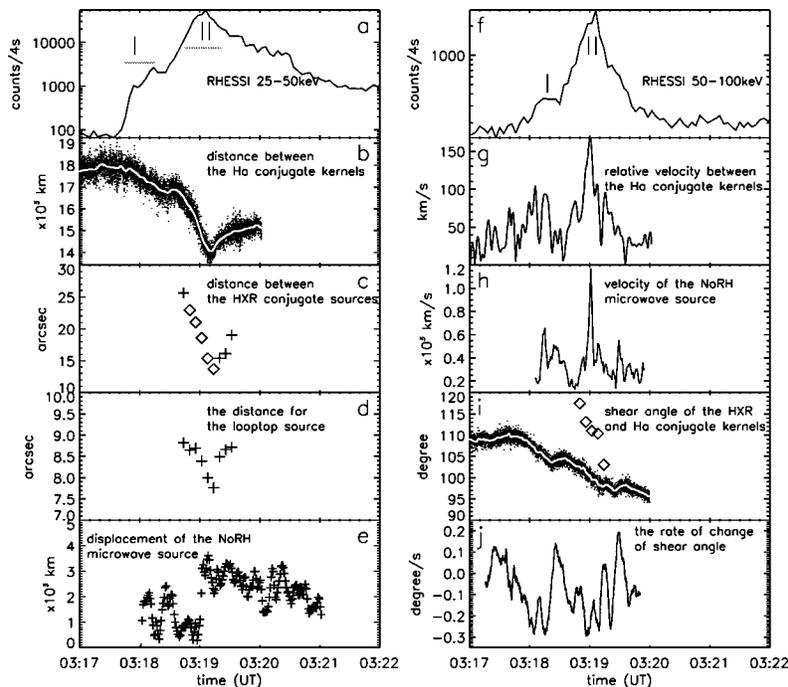[3] See http://plasma.pmo.ac.cn/preprint/haisheng/gy.mpeg.

Fig. 2.—Time profiles for a number of quantities. (*a, f*) *RHESSI* HXR counts for the energy bands of 25–50 and 50–100 keV; the time resolution is 4 s. (*b*) Centroid distance between the two conjugate Hα kernels, for which the cadence is ~40 ms. Each point represents the result from an Hα image. (*c*) Centroid distance of the two HXR conjugate sources. The points with the most accuracy are represented by diamonds. (*d*) The distance from the loop-top source to the line connecting the two HXR footpoints. (*e*) Displacement of the microwave source at 17 GHz observed by NoRH; the time cadence is 1 s. (*g*) Relative velocity of the two conjugate Hα kernels, obtained from the smoothed curve in panel *b*. (*h*) Velocity of the microwave source obtained from the smooth curve in panel *e*. (*i*) Shear angle obtained from HXR footpoints (*diamonds*) and Hα kernels (*dots*). (*j*) Rate of change of the shear angle obtained from the dotted curve in panel *i*.

the lower energy channel and a pair of FPs in the higher energy channel, as shown in Figure 1. With the aid of *RHESSI* maps, we further identify the Hα flaring kernels a1 and a2 as two conjugate kernels.

From Figure 1, it is not difficult to note that the two HXR FPs converge in the same way as the Hα kernels. We measured the distance between the two HXR FPs using a tool provided by *RHESSI* software (Image Flux in *RHESSI* GUI) to determine the centroids' positions. We also measured the distance from the centroid of the loop-top source to the line that connects the two HXR FPs. The time profiles for the distances are plotted in Figures 2*c* and 2*d*. We find that, during the converging motion of the Hα kernels, the HXR FPs also converge. The conventional separation motion for the HXR FPs appears only after the rising phase of HXR emissions. Meanwhile, the distance for the loop-top source shows a correlated time profile. The time profiles in Figures 2*b*–2*d* show an anticorrelation with HXR emissions.

In fact, converging motions of conjugate Hα and HXR kernels have been discussed in earlier literature. Sakao et al. (1998) mentioned the decreasing of the HXR FP separation for some flares. For the 2000 March 16 flare, Qiu et al. (2002) have noted that brightenings of kernel K1 are moving more or less toward K2, while K2 remains motionless. For the 2002 March 14 event investigated by Fletcher & Hudson (2002), the two conjugate HXR kernels have an obvious converging motion during the initial phase of the flare (Fig. 7 of Fletcher & Hudson 2002).

It is important to specify the moving direction of Hα kernels, HXR FPs, and the loop-top source. In Figure 1*g*, the centroid positions of the HXR sources are overlaid in a *Solar and Heliospheric Observatory*/Michelson Doppler Imager (*SOHO*/ MDI) magnetogram with colored boxes. The moving directions are shown with arrows. We can see that one FP moves almost

perpendicularly toward the neutral line (NL; in Fig. 1*g*), while the motion of another FP toward the NL shows a parallel component. The loop-top source moves mainly perpendicular to the NL, while having some motion along the NL. In Figure 1*h*, the contours of HXR FPs at two different time periods are specially overlaid to verify the direction of the FP motion. Furthermore, the positions of the centroids of the two Hα kernels at different time periods are plotted in Figure 1*h* with colored dots. It can be seen that the moving direction of the two Hα kernels is in good agreement with HXR FPs. Here, it is worth noting that, for FP a2, the HXR source has a more obvious motion than its Hα counterpart. The discrepancy may be due to different mechanisms for HXR and Hα FP emissions. In fact, heat conduction plays an important role in producing Hα emissions.

We computed the shear angle that is shown in Figure 1*h* using FP positions in HXR and Hα. In HXR we only use the points with the most accuracy (diamonds in Fig. 2*b*) to compute the shear angle. It turns out that the shear angle decreases during the converging motion (diamonds in Fig. 2*i*). Furthermore, the value of the shear angle computed from Hα also decreases. Actually, from Figure 1*h*, we can roughly see that the shear angle decreases during the converging motion. Here, it is worth noting that the motions of Hα and HXR FPs and EUV loops from strongly sheared to less sheared structure were also observed by Masuda et al. (2001) and Asai et al. (2003). According to Figure 1*g*, the overall neutral line has an S shape, which may serve as indirect evidence of a sheared magnetic field. In this event, the high cadence of the Hα observation enables us to compute the rate of change of the shear angle, which is plotted in Figure 2*j*. Comparing Figures 2*j* and 2*f*, we can see that the rate and the HXR light curve show similar behavior. Fine structures appear in the time profile of the rate, which may need further investigation.

The green contours overlaid in the Hα images of Figure 1 are

from microwave images constructed from NoRH observations at 17 GHz. Microwave images show a single source, which appears to be spatially correlated with the HXR loop-top source. We obtained the time profile of the displacement for the microwave source using the same method as we did for the Hα kernels. The displacement of the microwave source is defined as the distance from its position at 03:18:00. The time profile of the displacement is plotted in Figure 2e. In addition, we derived the velocity-time curve for the microwave source, which is given in Figure 2h. It is interesting to note that the curve exhibits an excellent correlation with the velocity-time curve for the Hα kernels. Since the imaging methods for Hα and microwave wavelengths are quite different, the correlation is perhaps surprising. However, they may reflect the fact that Hα and microwave emissions are from the same beam of high-energy electrons, although the emission mechanisms are quite different.

The magnitude of the converging velocity of the Hα kernels ranges from 50 to 150 km s^{-1}, while the converging velocity of the HXR footpoint sources is found to be ∼280 km s^{-1} by a linear fitting. The discrepancy in magnitude may be due to the fact that HXR footpoint emissions are more highly concentrated. The magnitude of the velocity for the microwave source is 6–7 times larger than that from Hα observations. The peak velocity of the microwave source is over 1000 km s^{-1}, equivalent to the Alfvén speed of the corona. Considering that the spatial resolution of NoRH is 10″ at 17 GHz, the magnitude of the velocity needs to be further investigated.

4. SUMMARY

We observed an M-class flare in the Hα blue wing with a cadence of 40 ms, and we compared it with HXR and microwave observations. The high-cadence observation enables us to get a detailed moving pattern of Hα kernels and detailed information on the behavior of the shear angle during the flare. In summary, we have the following results:

1. Both Hα and HXR observations show that a pair of conjugate kernels of the flare have a converging motion during the rising phase of the flare. The converging motion has a considerable perpendicular component to the magnetic neutral line. In particular, one kernel's converging is made perpendicular to the neutral line.

2. During the whole flaring process, the value of the shear angle of both Hα and HXR FPs decreases with time. The decreasing rate is correlated with HXR emissions. This may indicate a fast relaxation of a sheared magnetic field. Thus, the converging motion is the signature of a fast relaxation of the sheared magnetic field.

3. The velocity-time curve for the converging motion of Hα kernels shows an excellent correlation with that obtained from the microwave source. Both velocity-time curves show an impulsive signature and have a good correlation with the HXR light curve in the energy band of ≳50 keV. The impulsive phase of velocity occurs during the converging motion. It may provide additional evidence of the fast relaxation of the sheared magnetic field.

REFERENCES

Asai, A., Ishii, T. T., Kurokawa, H., Yokoyama, T., & Shimojo, M. 2003, ApJ, 586, 624
Asai, A., et al. 2004, ApJ, 611, 557
Bogachev, S. A., Somov, B. V., Kosugi, T., & Sakao, T. 2005, ApJ, 630, 561
Canfield, R. C., & Gayley, K. G. 1987, ApJ, 322, 999
Carmichael, H. 1964, in Proc. AAS-NASA Symp., The Physics of Solar Flares, ed. W. N. Hess (Washington, DC: NASA), 451
Fletcher, L., & Hudson, H. 2001, Sol. Phys., 204, 69
———. 2002, Sol. Phys., 210, 307
Forbes, T. G., & Lin, J. 2000, J. Atmos. Sol-Terr. Phys., 62, 1499
Grigis, P. C., & Benz, A. O. 2005, ApJ, 625, L143
Hirayama, T. 1974, Sol. Phys., 34, 323
Hurford, G. J., et al. 2002, Sol. Phys., 210, 61
Ji, H., Wang, H., Goode, P. R., Jiang, Y., & Yurchyshyn, V. 2004, ApJ, 607, L55
Kopp, R. A., & Pneuman, G. W. 1976, Sol. Phys., 50, 85
Krucker, S., Hurford, G. J., & Lin, R. P. 2003, ApJ, 595, L103
Lin, R. P., et al. 2002, Sol. Phys., 210, 3

Masuda, S., Kosugi, T., & Hudson, H. S. 2001, Sol. Phys., 204, 55
Nakajima, H., et al. 1994, Proc. IEEE, 82(5), 705
Priest, E., & Forbes, T. 2000, Magnetic Reconnection (Cambridge: Cambridge Univ. Press)
Qiu, J., Lee, J., Gary, D. E., & Wang, H. 2002, ApJ, 565, 1335
Saba, J. L. R., Gaeng, T., & Tarbell, T. D. 2001, in Multi-Wavelength Observations of Coronal Structure and Dynamics—*Yohkoh* 10th Anniversary Meeting, ed. P. C. H. Martens & D. Caufman (Amsterdam: Elsevier), 96S
Sakao, T., Kosugi, T., & Masuda, S. 1998, in Observational Plasma Astrophysics: Five Years of *Yohkoh* and Beyond, ed. T. Watanabe, T. Kosugi, & A. C. Sterling (Dordrecht: Kluwer), 273
Somov, B. V., Kosugi, T., Bogachev, S. A., Sakao, T., & Masuda, S. 2005, Adv. Space Res., 35, 1700
Sturrock, P. A. 1966, Nature, 211, 695
Sui, L., & Holman, G. D. 2003, ApJ, 596, L251
Švestka, Z., & Cliver, E. W. 1992, in IAU Colloq. 133, Eruptive Flares, ed. Z. Švestka, B. V. Jackson, & M. E. Machado (New York: Springer), 1
Wang, H., Qiu, J., Jing, J., & Zhang, H. 2003, ApJ, 593, 564